

The Evolution of Radio-Loud Quasars at High Redshift

I. M. Hook, P. A. Shaver

European Southern Observatory, Karl Schwarzschild Strasse-2, D85748 Garching b. München, Germany

R. G. McMahon

Institute of Astronomy, Madingley Road, Cambridge, U.K.

Abstract. We present results from two surveys for radio-loud quasars. These are (1) a northern survey reaching $S_{5\text{GHz}} = 0.2\text{Jy}$ and (2) the Parkes QSO survey reaching $S_{2.7\text{GHz}} = 0.25\text{Jy}$, which together cover most of the sky. Both surveys use digitised plate material to identify the majority of the radio sources and CCD images to identify the optically fainter sources. The northern survey was targeted specifically at $z > 3$ QSOs and has produced more than 20, one of which, at $z = 4.72$, is the most distant radio source known. This sample is identified to the POSS-I plate limit (20 mag) over an area of 3.7sr, or 12 000 sq deg. With the addition of CCD identifications, an effective sub area of 2400 sq degrees is 97% identified. In the South the Parkes QSO survey now has complete redshift information for all 442 flat-spectrum quasars. These cover the redshift range $z \sim 0$ to $z \sim 4.5$ and show a clear drop-off in space density at redshifts above 3. The form of this decline is remarkably similar in form to that seen in optically-selected samples of quasars. Since radio emission is unaffected by dust this implies that dust has a minimal effect on the observed drop-off seen in optical samples. Analysis of our radio-selected samples suggests that the decline in space density at high redshift is more pronounced for less powerful radio sources. We are planning a new survey that will be sensitive to bright quasars with redshifts up to 6.

1. Introduction

The mere existence of QSOs and their host galaxies at high redshift places interesting constraints on theories of large-scale structure and galaxy formation (Haehnelt & Rees 1993, Efsthathiou & Rees 1988). However, recent optical surveys have produced conflicting results for the QSO space density at high redshift, due to the complicated selection effects introduced when picking out high-redshift QSOs from more numerous galactic stars with similar optical colours. *Radio*-based selection methods have the advantage of simpler selection criteria. Also, since radio emission is unaffected by dust, the intrinsic evolution of the QSO population can be observed, unaffected by obscuration. QSOs found in radio-based surveys provide an unbiased (by the effects of dust) sam-

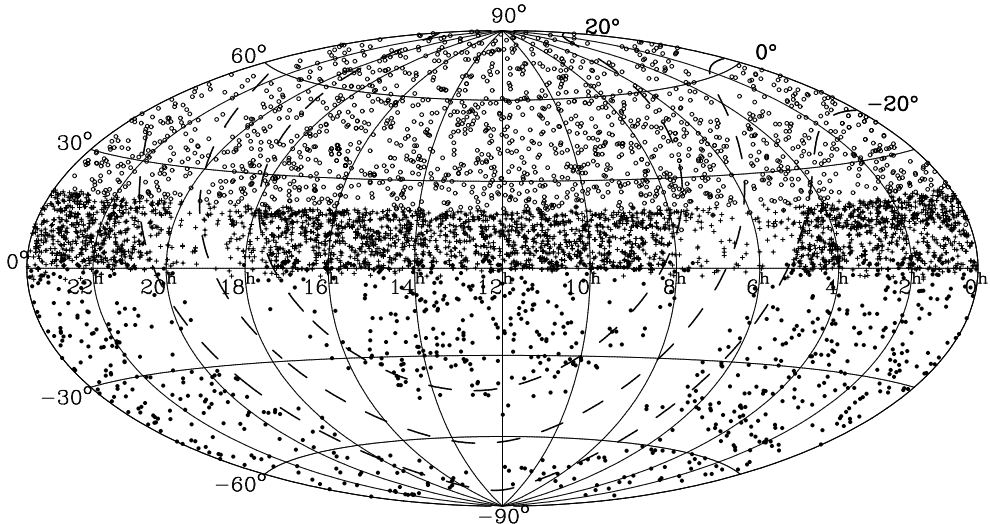


Figure 1. Sky coverage of the three radio-samples that form the basis of our surveys. These are the 0.2Jy flat-spectrum sample of Patnaik et al (1992) for $\delta > 20^\circ$, the 0.1Jy MG-VLA sample (Lawrence et al 1986) in the region $0^\circ < \delta < 20^\circ$ and flat-spectrum sources from the Parkes catalogue in the South. Almost the whole sky (excluding the galactic plane, shown by the dashed lines) is covered to a depth of 0.25Jy or fainter. Only regions that are complete to a well-defined flux limit are used for the analysis of quasar evolution.

ple of damped Ly- α absorption systems that can be used to study chemical abundances to the highest observable redshifts.

2. Two surveys for radio-loud quasars

Since high-redshift quasars are rare, surveys to reach $z > 3$ must cover a large area. We are carrying out two surveys using three radio samples that cover most of the sky to a limit of 0.25Jy or fainter (see Figure 1 and caption). The northern survey uses the 0.2Jy flat-spectrum sample of Patnaik et al (1992) and the 0.1Jy MG-VLA sample (Lawrence et al 1986), which together contain more than 4400 sources. The southern survey uses the revised Parkes catalogue (Wright & Otrupcek, 1990). Since these samples are defined at high frequency (5GHz for the northern samples and 2.7GHz for the Parkes sample), they contain a high fraction of core-dominated flat-spectrum sources, usually identified with quasars. Moreover, spectral index information is available for all the sources, allowing us to select flat-spectrum objects. In addition the sources have accurate positions from the VLA and/or the Australia telescope, which are necessary for making unambiguous optical identifications.

The first stage of optical identification is carried out using digitised sky-survey plates. CCD images are then obtained for the fainter sources. Since the northern survey was aimed at finding high-redshift quasars, only the optically red, stellar identifications were followed up spectroscopically. For the Parkes

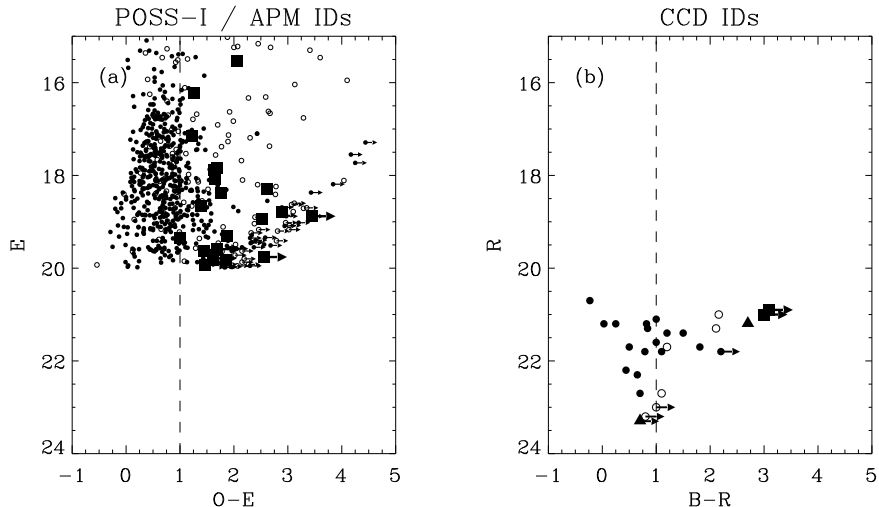


Figure 2. Colour-magnitude diagrams for flat-spectrum sources with $S \geq 0.2\text{Jy}$ from the northern survey. (a) APM/POSS-I identifications covering an area of 12 000 sq deg. (b) CCD identifications for a 2400 sq deg sub-area. Stellar sources are shown as filled circles and open circles represent galaxies. The $z > 3$ quasars are shown as squares. The two triangles represent red, stellar objects that do not yet have a spectrum. The dashed lines show the colour limits used to define the spectroscopic sample.

sample redshifts were obtained for all the stellar identifications. Details of the two surveys are given below.

2.1. The Northern High-redshift Radio-loud QSO Sample.

POSS-I plates in the E and O bands, scanned by the APM (Automated Plate Measuring facility, Cambridge U.K.), were used to identify flat-spectrum ($\alpha \geq -0.5$, $S \propto \nu^\alpha$) sources with $S_{5\text{GHz}} \geq 0.2\text{Jy}$ to the plate limit of $E = 20\text{mag}$ over an area of 3.7sr (12 000 sq deg). Their colour magnitude diagram is shown in Figure 2a. Since high-redshift quasars have redder optical colours than their low-redshift counterparts due to absorption by intervening Ly- α , only red ($O - E \geq 1.0$), stellar identifications were followed up spectroscopically. This resulted in the discovery of 20 $z > 3$ quasars (Hook 1994, Hook et al 1995, 1996). Another 5 $z > 3$ QSOs with radio fluxes $0.1\text{Jy} \leq S_{5\text{GHz}} \leq 0.2\text{Jy}$ were found in the region covered by the MG-VLA sample.

About 16% of the radio sources remained unidentified after this stage and B and R-band CCD identifications are being obtained for these. So far ~ 40 have been observed and a colour-magnitude diagram for those detected in the R-band is shown in Figure 2b. Combining the POSS-I and CCD identifications plus observations of these radio sources from the literature (including the identification of one source as a QSO with $z = 3.82$, Vermeulen et al 1996), an effective

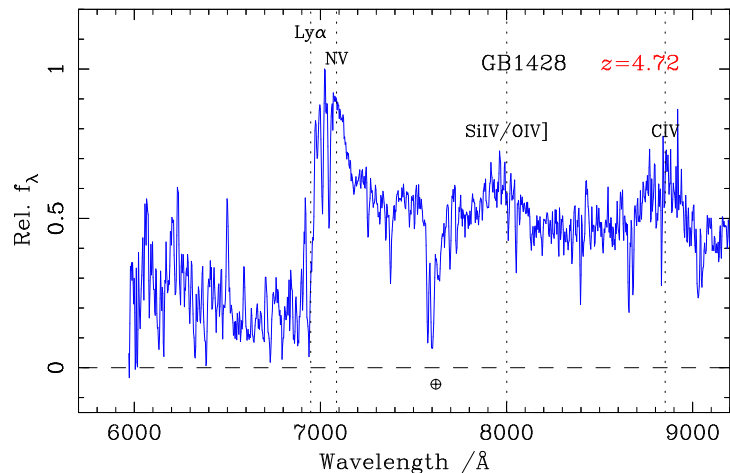


Figure 3. The optical spectrum of GB1428, the most distant known radio source and the third highest redshift QSO known (Hook & McMahon 1998). This object was discovered among CCD identifications of flat-spectrum radio sources with $S \geq 0.2\text{Jy}$. The spectrum shows unusually weak emission lines for a radio-loud quasar, consistent with the scenario that it is beamed (Fabian et al 1997). Note that the spectrum has not been corrected for the sky absorption feature at $\sim 7600\text{\AA}$.

area of 2400 sq deg is now 97% identified. 10 objects are still not identified to a limit of $R \sim 23\text{mag}$. Two new $z > 4$ QSOs were found during spectroscopy of the 10 reddest CCD identifications. One of these, at $z = 4.72$ is the highest redshift radio source known (Hook & McMahon 1998). Its spectrum is shown in Figure 3. It is also the highest redshift X-ray source known and is probably strongly beamed (Fabian et al 1997).

We are able to compute the luminosity function of radio-loud QSOs at high redshift using the $z > 3$ QSOs discovered among the POSS and CCD identifications. The distribution of the QSOs on the radio-luminosity versus redshift plane is shown in Figure 4 along with flat-spectrum QSOs at $z < 3$ from Dunlop & Peacock (1990). The binned luminosity function for these two data sets is shown in Figure 5. Notice that the luminosity function at $z > 3$ is lower than that at $z \sim 2$, particularly for sources of lower radio luminosity.

2.2. The Parkes QSO Sample.

Initial identifications of flat-spectrum sources ($\alpha \geq -0.4$) from the Parkes catalogue were made by Shaver et al (1996a) using COSMOS scans of UKST plates to a limit of $B_J \sim 22\text{mag}$. CCD identifications were obtained for the remaining optically-fainter sources. Since all the stellar sources have been identified in the B band, Shaver et al (1996a) were able to conclude there are no $z > 5$ QSOs in the sample (see the limit in Figure 6) and hence there must be a drop-off in the space density of radio-loud quasars at $z > 3$.

The next stage of this study, namely to obtain redshifts for a complete subsample of 442 stellar identifications (quasars) with $S_{2.7\text{GHz}} \geq 0.25\text{Jy}$, has recently been completed. The most distant QSO found in this sample has $z = 4.46$ (Shaver et al 1996b). Figure 6 shows a preliminary analysis of space density

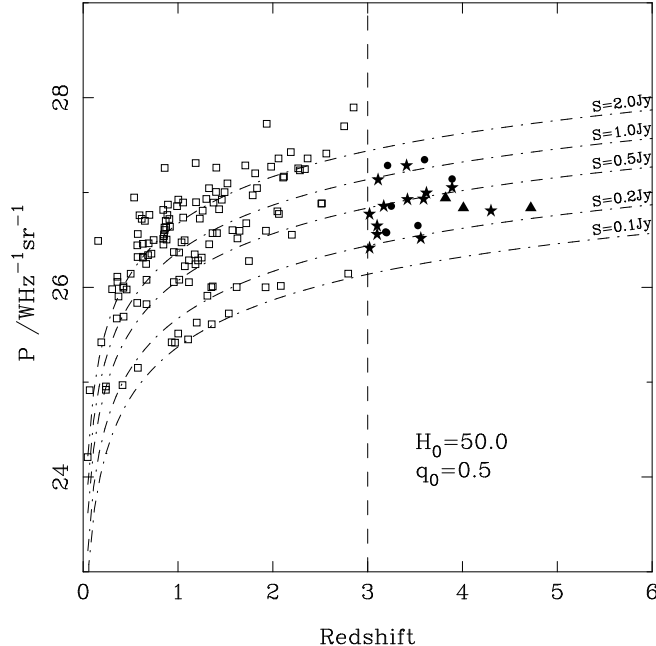


Figure 4. Distribution of $z > 3$ radio-loud QSOs with $S \geq 0.2\text{Jy}$ from the northern sample (solid symbols) on the radio power vs redshift plane, plotted with flat-spectrum QSOs with $z < 3$ from Dunlop & Peacock 1990 (open squares). Circles are QSOs from the MG-VLA sample; stars represent QSOs from the $S \geq 0.2\text{Jy}$ flat-spectrum sample identified on APM/POSS-I scans and triangles are sources from the same radio sample identified on CCD images.

as a function of redshift for objects with radio luminosity greater than $P_{\text{lim}} = 7.2 \times 10^{26} \text{WHz}^{-1} \text{sr}^{-1}$, corresponding to the flux limit of the sample at $z = 5$ (for $H_0 = 50 \text{kms}^{-1} \text{Mpc}^{-1}$ and $q_0 = 0.5$). The Figure shows that the decline in space density of luminous Parkes QSOs at $z > 3$ has a remarkably similar form to that seen in optically-selected samples of QSOs. Since the radio sample is unaffected by dust this suggests that dust has a minimal effect on the observed drop-off in space density of optically-selected QSOs. This also has implications for the effect of dust on recent measurements of the star formation rate from high-redshift galaxies. We are working on quantifying this result in the context of the obscuration models of Fall & Pei (1993).

3. QSO Evolution & A New Large Survey

The results from the above surveys suggest that the peak in QSO space density occurs at higher redshifts for stronger sources (Fig 7). Thus a survey to reach higher redshifts should concentrate on relatively bright objects and cover a large area, rather than reaching very faint limits over a small region.

We are planning a very large survey for $z > 4$ QSOs, making use of new wide-area datasets. The survey covers 6000 sq deg and is based on flat-spectrum sources with $S_{5\text{GHz}} \geq 50 \text{mJy}$ from the 5GHz PMN sample. The 1.4GHz NRAO-VLA Sky Survey (NVSS, Condon et al 1994), which now covers the whole sky

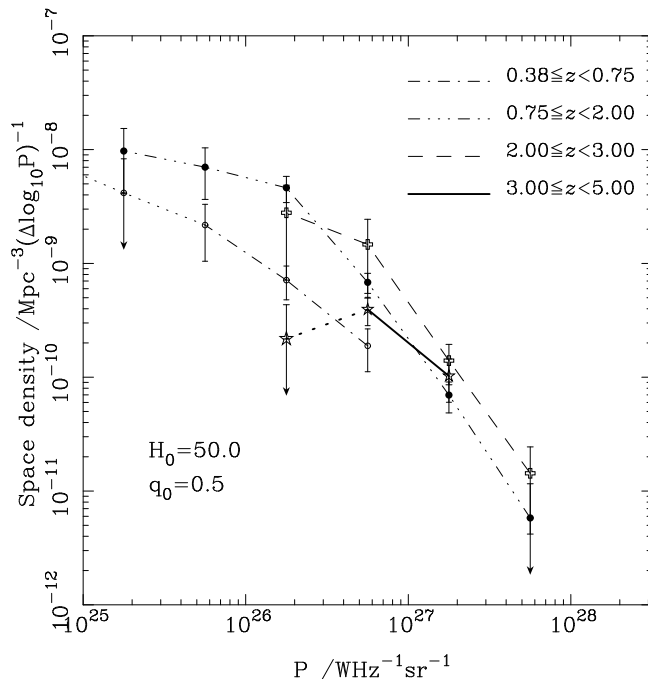


Figure 5. The luminosity function of flat-spectrum QSOs as determined from the data shown in Figure 4. Notice that the space density at $z > 3$ is lower than at $z \sim 2$, particularly for weaker sources. Downward arrows indicate that the error bar extends to zero since there is only one point in these bins.

north of -40° , will provide spectral index information and the accurate positions needed to make unambiguous optical identifications. The UKST I-band survey of the southern sky is now nearing completion and the plates are being scanned at the APM. As in the northern survey described above, candidate high-redshift QSOs will be selected based on positional coincidence, red optical colour and ‘stellar’ image classification. By using I-band plates this survey is sensitive to bright QSOs out to $z \sim 6$. Extrapolating our previous results to 50mJy, 8 – 24 radio-loud objects with $z > 4$ should be found (2 – 6 times the number currently known) plus up to 2 with $z > 5$.

4. Conclusions

There are 4 main conclusions from this work.

- Radio surveys are efficient for finding high-redshift QSOs. There are now many tens of $z > 3$ radio-selected quasars known including GB1428 at $z = 4.72$, the third highest redshift quasar known.
- The space density of radio-selected QSOs shows a turnover at high-redshift ($z > 3$). Since radio emission is unaffected by dust, this decline at high redshift is not an effect of obscuration.
- The decline in space density seen at high redshift has a similar form to that of optically-selected QSOs.

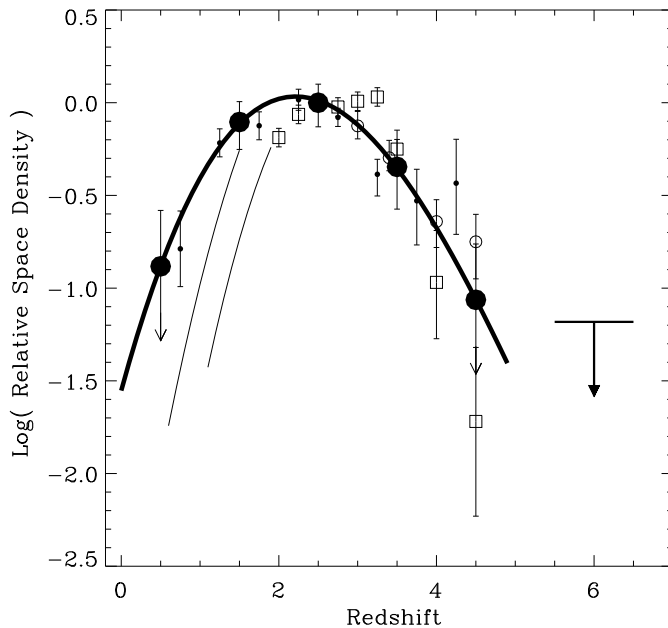


Figure 6. Space densities, normalized to $z \sim 2 - 3$ and plotted as a function of redshift, for the Parkes flat-spectrum radio-loud quasars with $P_{\text{lim}} > 7.2 \cdot 10^{26} \text{ W Hz}^{-1} \text{ sr}^{-1}$ (\bullet). The number of such objects found in the individual redshift ranges are 1 ($0 < z < 1$), 12 ($1 < z < 2$), 15 ($2 < z < 3$), 6 ($3 < z < 4$), and 1 ($4 < z < 5$); the error bars correspond to $\pm\sqrt{N}$. The thick curve is a cubic fit to these data. The upper limit shown in the redshift range $5 < z < 7$ is taken from Shaver et al (1996a). For comparison, similarly normalized space densities are also shown for the optically-selected quasar samples of Warren *et al.* (1994) (\square), Schmidt *et al.* (1995) (\circ), and Hawkins & Véron (1996) (\bullet). The thin lines represent luminosity functions from Boyle (1991) and Hewett *et al.* (1993) used by Warren *et al.* and Schmidt *et al.* respectively as lower-redshift continuations of their high-redshift space densities.

- The two previous results lead to the conclusion that the effect of dust on the observed QSO drop-off is minimal.

References

- Boyle B.J. in *Relativistic Astrophysics, Cosmology and Fundamental Physics* (eds Barrow J.D. et al), Ann. NY Acad Sci. 1991, 647, 14
- Condon, J. J. et al., 1994 *ADASS III*, ASP, ed. Crabtree et al., 155
- Dunlop J.S., Peacock J.A., 1990, MNRAS, 247, 19
- Fabian A.C., Brandt W.N., McMahon R.G., Hook I.M., 1997, MNRAS, 291, L5
- Fall S.M., Pei Y., 1993, ApJ, 402, 479
- Efstathiou G., Rees, M. 1988, MNRAS, 230, 5
- Haehnelt M., Rees M. 1993 MNRAS, 263, 168
- Hawkins M.R.S, Véron P., 1996, MNRAS, 281, 348

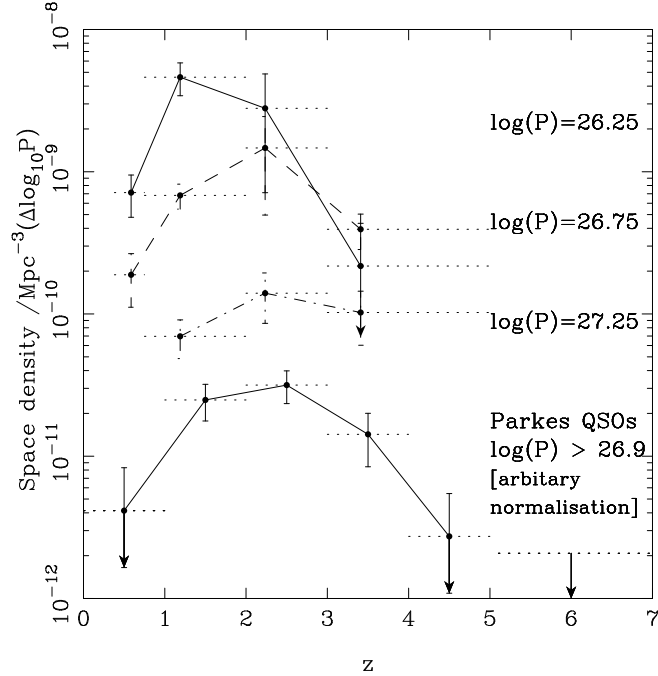


Figure 7. Space density as a function of redshift for sources with various radio luminosity P . The top three curves are from the northern sample combined with data from Dunlop & Peacock (1990) -see caption of Figure 4. The lower curve is from the Parkes sample (see Fig. 6) and is plotted with arbitrary normalisation. The dotted lines show the extent of the redshift bin used to compute each point.

- Hewett P.C. Foltz C.B., Chafee F.H., 1993, ApJ, 406, L43
Hook I. M., 1994, PhD thesis, Cambridge, U.K.
Hook I.M., McMahon R.G., Patnaik A.R., Browne I.W.A., Wilkinson P.N, Irwin M.J., Hazard C., 1995, MNRAS, 273, 63L
Hook I.M, McMahon R.G., Irwin, M. J., Hazard, C., 1996, MNRAS, 282, 1274
Hook I. M, McMahon R. G., 1998, MNRAS, in press
Lawrence C. R., Bennett C. L., Hewitt J. N., Langston G. I., Klotz S. E., Burke B. F., 1986, ApJS, 61, 105
Patnaik A. R., Browne I. W. A., Wilkinson P. N., Wrobel J. M., 1992, MNRAS, 254, 655
Shaver P. A., Wall J. V., Kellermann K. I., Jackson C. A., Hawkins M. R. S., 1996a, Nat, 384, 439
Shaver P. A., Wall J.V., Kellerman K.I., 1996b, MNRAS, 278, L11
Schmidt M. Schneider D.P., Gunn J.E., 1995, AJ, 110, 68
Vermeulen R., Taylor G. B., Readhead A. C. S., Browne I. W. A., 1996, AJ, 111, 1013
Warren S. J., Hewett P. C., Osmer P. S., 1994, ApJ, 421, 412
Wright A. E., Otrupcek, R. E., 1990 (Australia Telescope National Facility, CSIRO).